Current Biology, Volume *27*

Supplemental Information

Activation of a Plant NLR Complex through Heteromeric Association with an Autoimmune Risk Variant of Another NLR

Diep T.N. Tran, Eui-Hwan Chung, Anette Habring-Müller, Monika Demar, Rebecca Schwab, Jeffery L. Dangl, Detlef Weigel, and Eunyoung Chae

Supplemental Figures

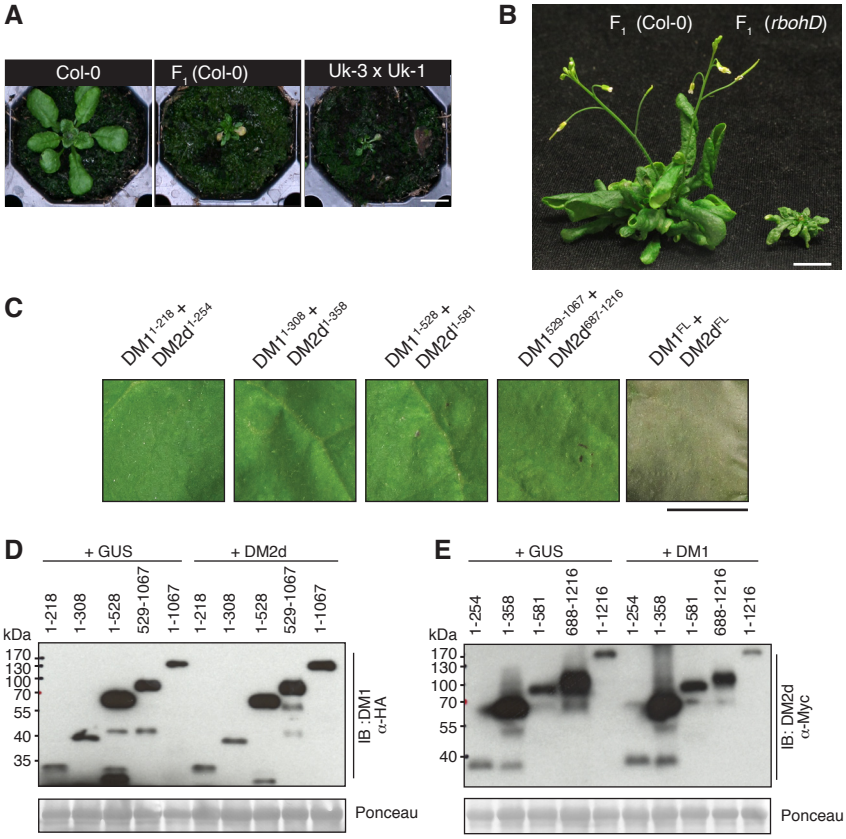

Figure S1. Recapitulation of hybrid necrosis in transgenic *A. thaliana*. Related to Figure 1

(A) Comparison of 30-day old F_1 hybrid for *gDM1-HA* x *gDM2d-Myc* in Col-0 wild-type background (middle) and Uk-3 x Uk-1 hybrid (right) [S1] grown at 16°C. Scale bar equals 1 cm.

(B) 55-day old *gDM1-HA* x *gDM2d-Myc* F_1 hybrids in Col-0 wild-type (left) and *rbohD* mutant (right) backgrounds grown at 16°C. The F_1 hybrid in Col-0 background eventually flowered and set seeds, but the one in *rbohD* background did not. Scale bar equals 1 cm.

(C) Representative effects of DM1/DM2d combinations (see Supplemental Experimental Procedures for construct information) in *N. benthamiana* at 4 dpi. Positional information is in Figure 2A-B. Scale bar equals 1 cm.

(D-E) Protein blots for experiments shown in (C), with samples taken at 2 dpi. Ponceau-S staining shown to indicate loading.

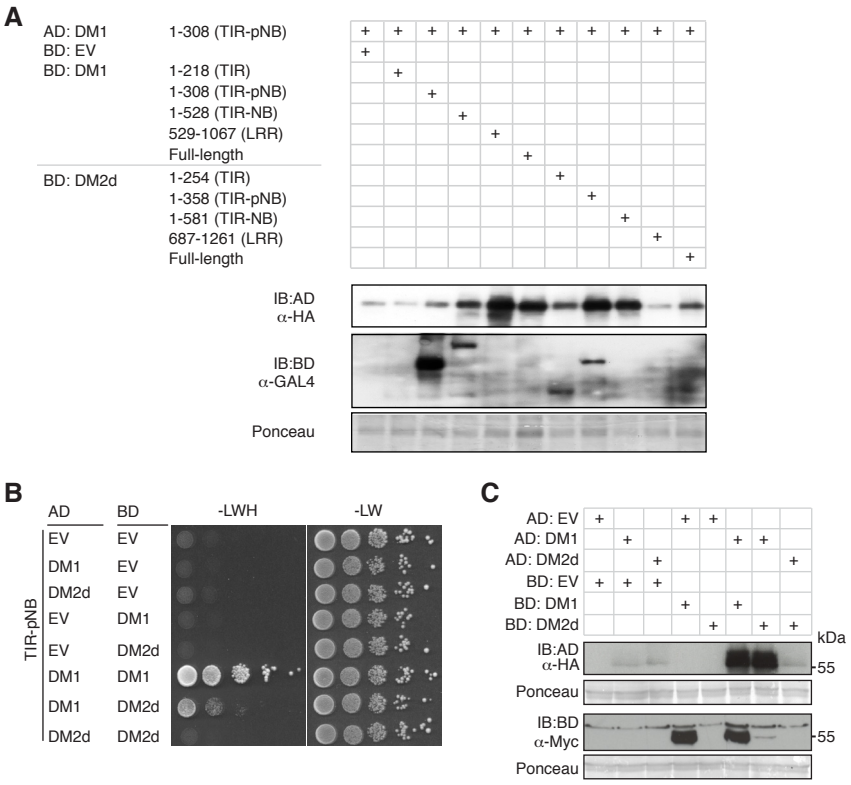

Figure S2. Y2H assay of DM1 and DM2d TIR-pNB fragments. Related to Figure 3

(A) Protein blot of samples shown in Figure 3A. TIR-pNB fragments of both DM1 and DM2d were well expressed, validating the usage of the fragments for further Y2H analyses. Neither LRR nor full-length proteins of DM1 and DM2d were detected. Despite non-detectable levels of TIR and full-length of DM1, Y2H interactions were positive.
AD: GAL4 activation domain, BD: GAL4 DNA-binding domain, EV: empty vector.
(B) Y2H analysis of DM1 and DM2d TIR-pNB fragments.
(C) Protein blot of samples shown in (B). DM2d TIR-pNB fused to BD was not detectable when DM1 TIR-pNB was not present.
Ponceau-S staining shown to indicate loading in (A) and (C).

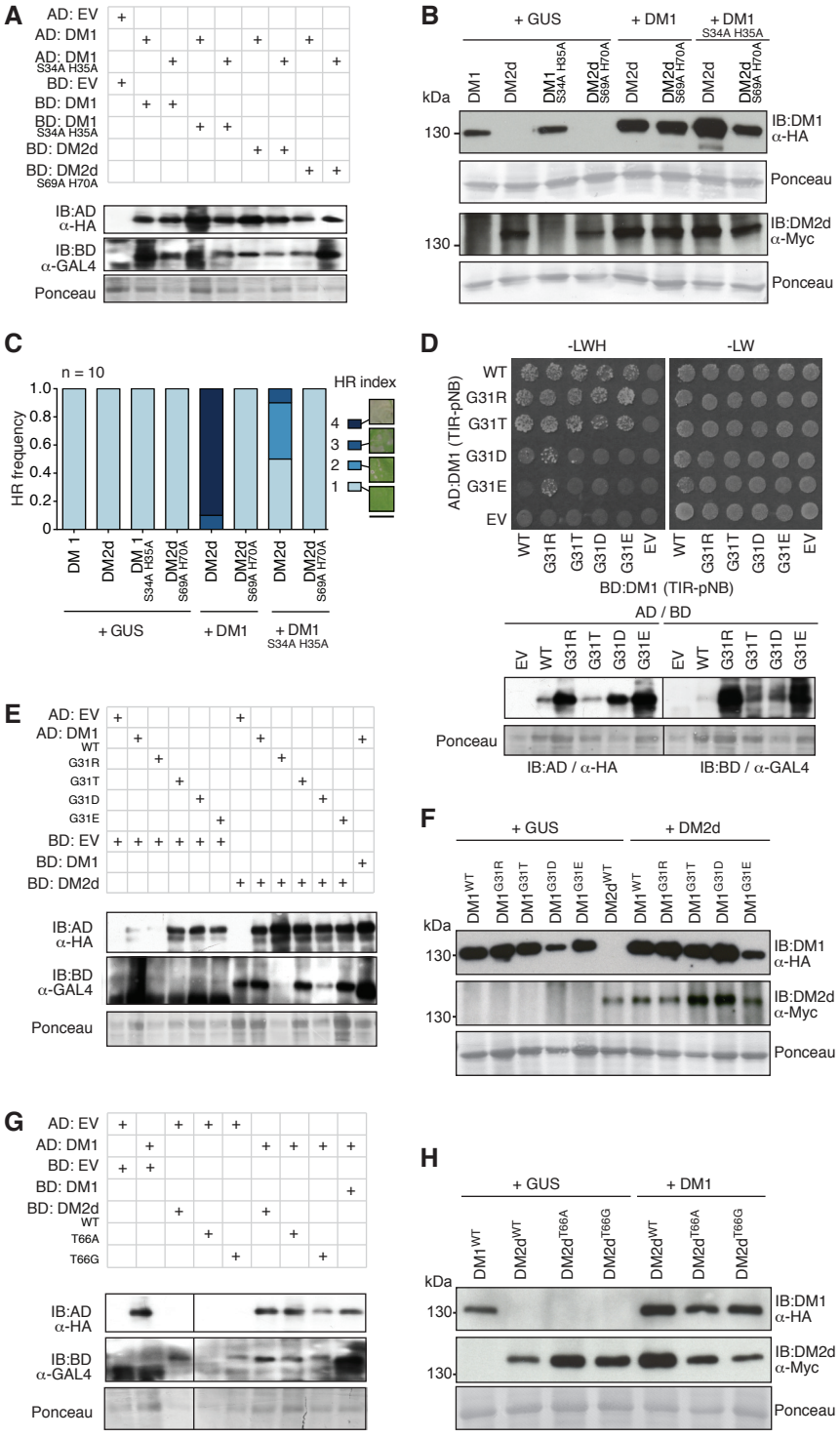

Figure S3. Characterization of DM1 and DM2d SH-motif mutants. Related to Figure 4

(A, E, G) Protein blots for Y2H shown in Figures 4A, 4C and 4E, respectively. All the DM1 and DM2d variants were expressed in yeast cells. AD fused proteins visualized with anti-HA blots and BD fused proteins with anti-GAL4 (DBD) blots.
(B, F, H) Protein blots for experiments shown in Figures 4B, 4D and 4F, respectively. All the DM1 and DM2d variants were expressed in *N. benthamiana*. Samples were taken at 2 dpi.

(C) Semi-quantitative scoring for HR in *N. benthamiana*. The HR index represents a percentage of area exhibiting HR in the infiltrated area as shown in the examples on the right at 4 dpi: 1 (no HR in field of view), 2 (less than 20% HR), 3 (20 to 60% HR) and 4 (over 60% HR). Scale bar equals 1 cm.
(D) Y2H assays with DM1 TIR-pNB fragments having different G31 substitutions and protein blots from the yeast cells carrying indicated constructs.
Ponceau-S staining shown to indicate loading (A, B, D-H)

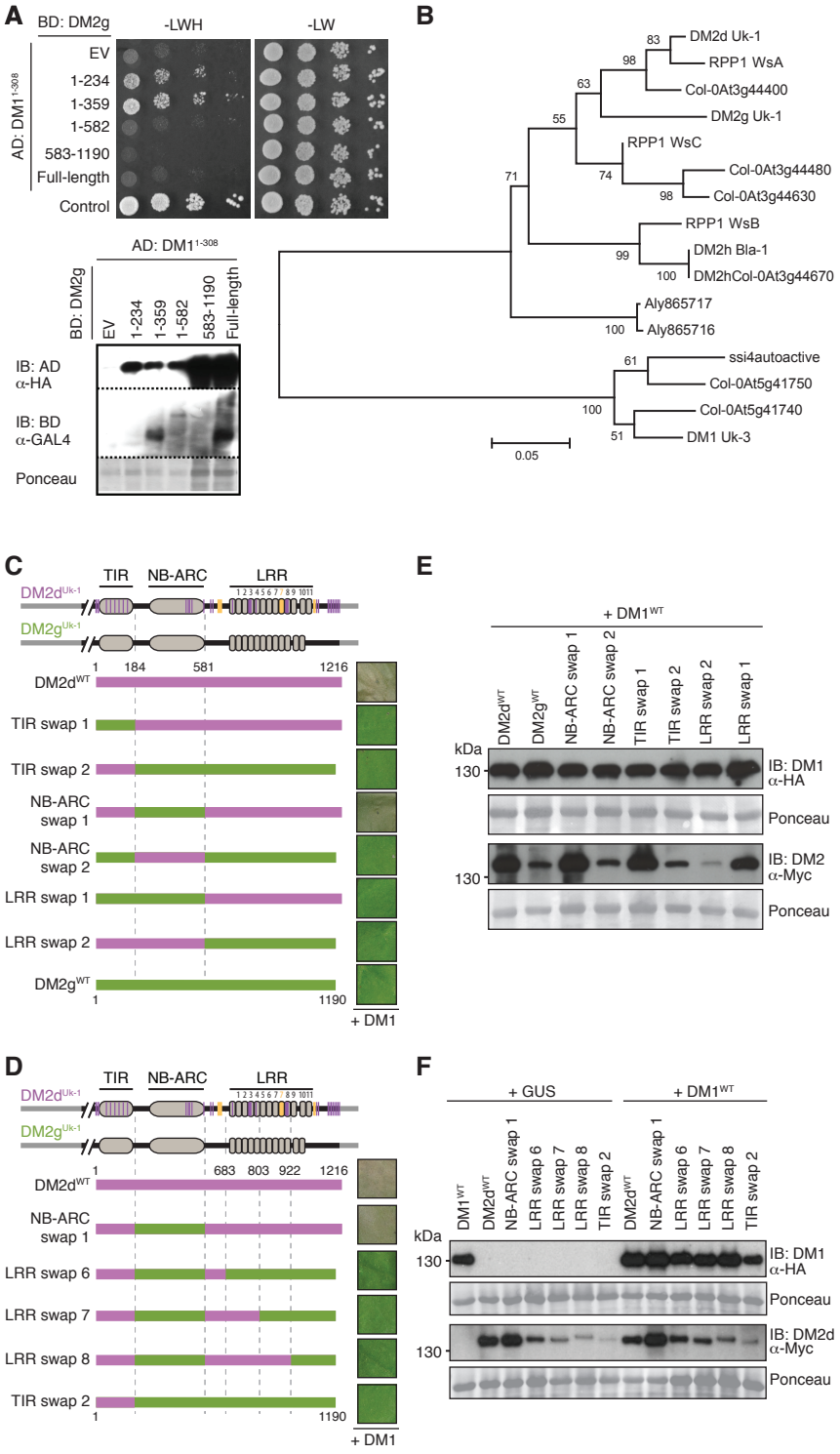

Figure S4. Domain swapping to localize functional differences between DM2d and DM2g. Related to Figure 5

(A) Y2H assay using DM1 TIR-pNB and DM2g fragments; the interaction is similar to that between DM1 and DM2d (see Figure 3A). Protein blots show LRR (583-1190) and full-length of DM2g are not detectable.

(B) Phylogeny constructed from amino acid sequences of TIR domains of DM2/RPP1 and DM1 proteins, using the Neighbor-Joining method based on the Kimura 2-parameter model implemented in MEGA5.
(C-D) Domain swaps between DM2d and DM2g. Purple vertical lines indicate SNPs and orange bars indels. Green bars indicate DM2g fragments. The numbers refer to positions in DM2d. *N. benthamiana* leaves are shown on right (4 dpi).
(E-F) Protein blots for experiments shown in Figures S4C and S4D, with samples collected 2 dpi. Ponceau-S staining shown to indicate loading.

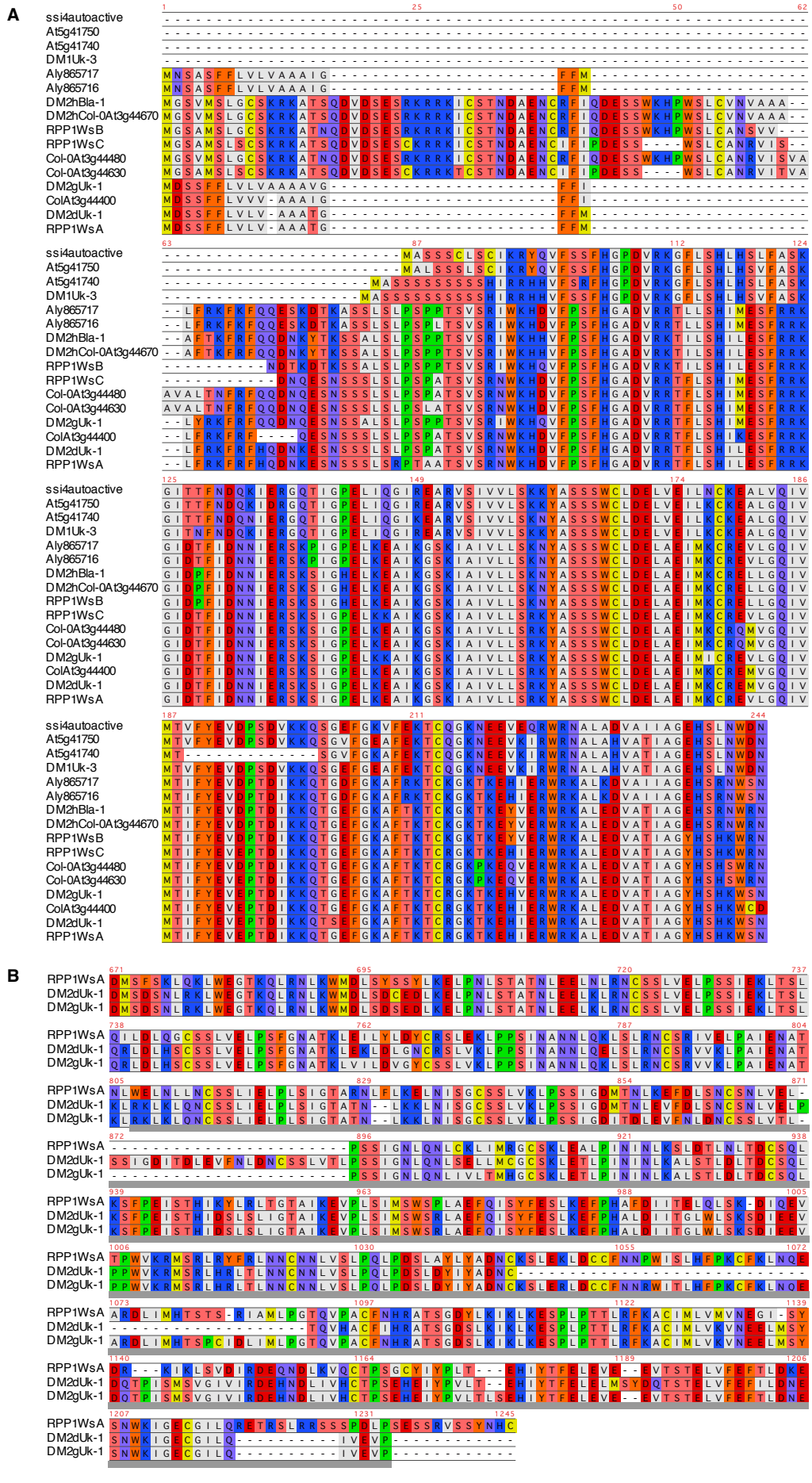
A
ssi4autoactive
At5g41750
At5g41740
DM1Uk-3
Aly865717
Aly865716
DM2hBla-1
DM2hCol-0At3g44670
RPP1WsB
RPP1WsC
Col-0At3g44480
Col-0At3g44630
DM2gUk-1
ColAt3g44400
DM2dUk-1
RPP1WsA
B
RPP1WsA
DM2dUk-1
DM2gUk-1

Figure S5. Amino acid alignment of TIR domain and LRR domain from multiple alleles of DM2/RPP1. Related to Figure 5

(A) Amino acid alignment of the N-terminal region sequences of DM1 and DM2/RPP1 alleles. DM2h types, RPP1 WsB/WsC, and their homologs from Col-0 (At3g44630, At3g44480) have the extended N-terminus, which was referred to N-TIR by [S2].
(B) Amino acid alignment of the C-terminal region sequences of DM2d/g and RPP1WsA, including LRR domains. Differences between DM2d and DM2g in the functionally critical region defined by domain swaps (underlined with gray bars) are mostly located close to indels: six polymorphisms in the duplicated LRR7 region in DM2d (853, 855, 860, 862, 866, 869), four (905, 906, 908, 910) C-terminal to the LRR7 duplication, two (1095, 1099) after the large indel (1045-1091), and small indels (1176-1177 and 1189-1190, 1192) at the extended C-terminus.

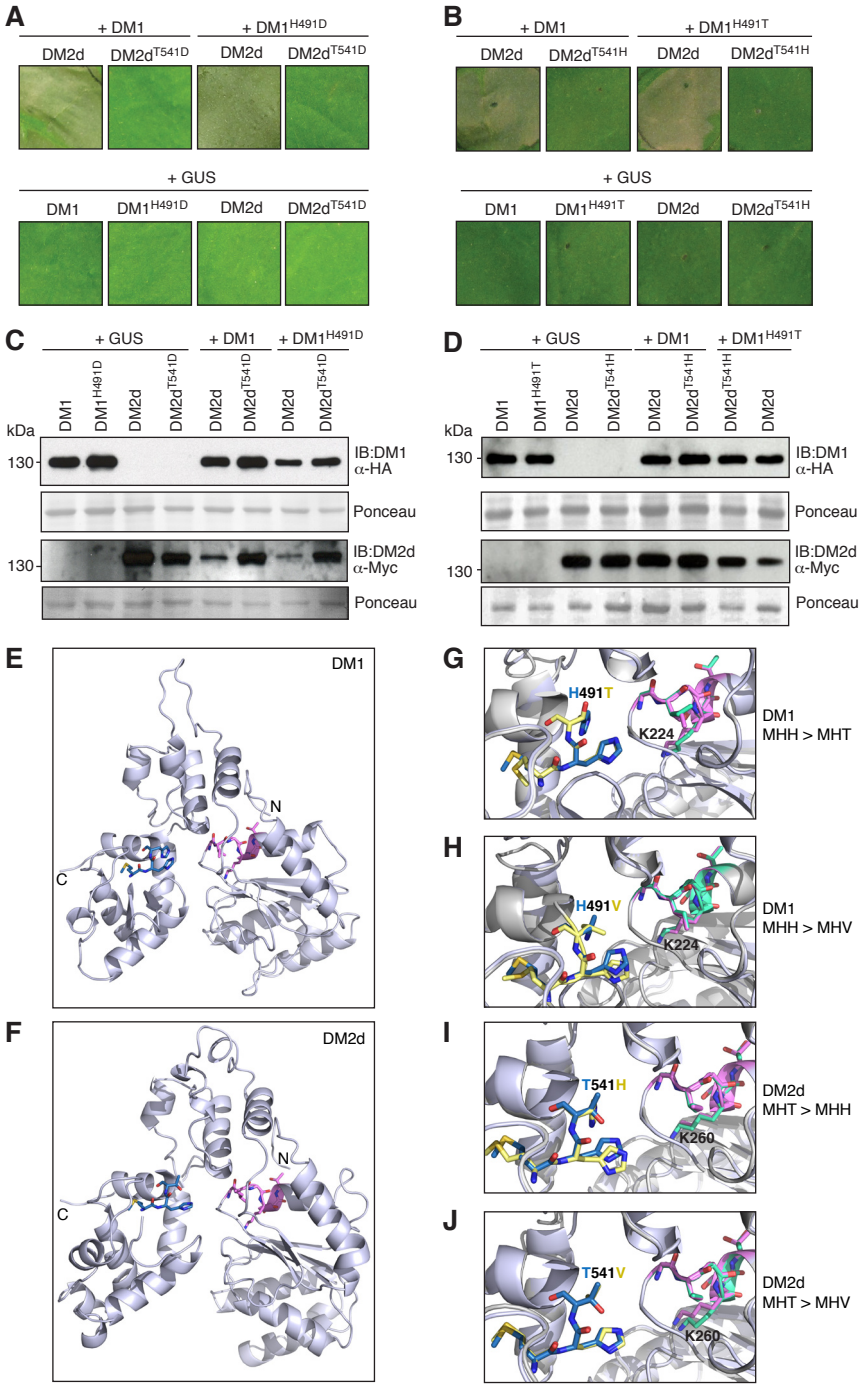

Figure S6. Additional characterization of DM1 and DM2d MHD-like motifs. Related to Figure 6

(A, B) DM1^{H491D}, DM1^{H491T}, DM2d^{T541H} and DM2d^{T541D} mutants were transiently co-expressed in *N. benthamiana* with the indicated partners. DM1^{H491D} and DM1^{H491T} functioned similar to the wild-type version, but DM2d^{T541D} and DM2d^{T541H} did not. HR phenotypes were scored at 4 dpi.

(C-D) Protein blots for experiments shown in (A, B), with samples taken 2 dpi. Ponceau-S staining shown to indicate loading.

(E-F) Homology modeling of NB-ARC domains of DM1 (E) and DM2d (F) based on that of mNLRC4 [S3] using the PHYRE2 web application [S4]. The P-loop and MHD-like motifs are highlighted in pink and blue.
(G-J) Superimposed models of MHD-like motifs in wild type and mutants. For wild-type proteins, P-loop motifs highlighted in pink and MHD-like motifs in blue. For mutated proteins, P-loops highlighted in green and MHD-like motifs in yellow.

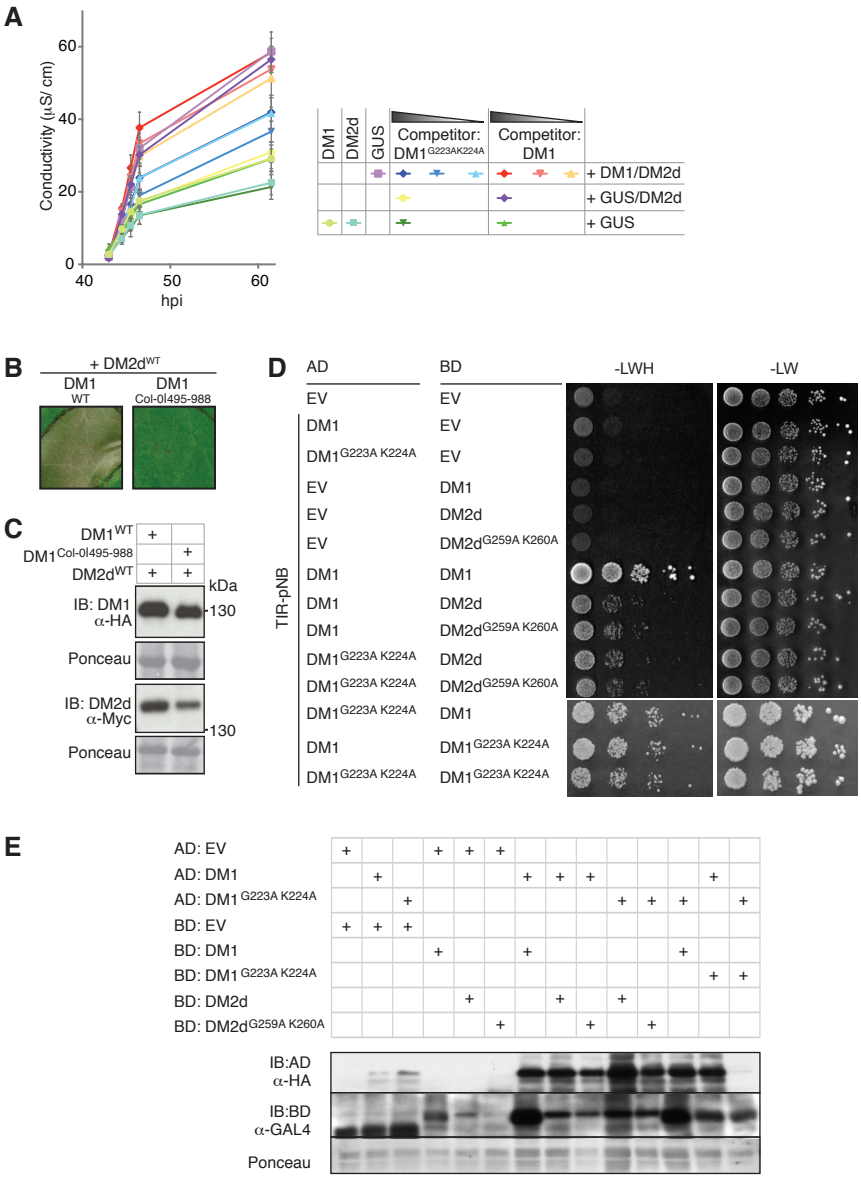

Figure S7. Additional characterization of DM1 and DM2 variants used in competition assays. Related to Figure 7

(A) Ion leakage as an indication of HR with wild-type or P-loop mutant DM1 competitor. Values are means ± SEM (n=6). hpi, hours post-infiltration

(B) HR at 4 dpi triggered by coexpression of DM1, but not DM1$^{Col\text{-}0|495\text{-}988}$ with DM2d in *N. benthamiana*. Scale bar equals 1 cm.

(C) Protein blots for experiment in (B), with samples taken at 2 dpi. Ponceau-S staining shown to indicate loading.

(D) Y2H analysis of TIR-pNB fragments of DM1 and DM2d carrying P-loop mutations. Both mutants behave like their wild-type counterparts.

(E) Protein blots for Y2H shown in (D). All the P-loop mutants were expressed comparable to their wild-type counterparts. Ponceau-S staining shown to indicate loading.

Supplemental Table

Table S1. Mutants used. Related to Figure 1

Mutant	Accession	Reference	Means of validation
eds1-1	Ws-0	[S5]	Sanger sequencing of PCR product
rar1-21	Col-0	[S6]	Sanger sequencing of PCR product
sgt1b	Col-0	[S7]	Sanger sequencing of PCR product
rbohD (SALK_074825)	Col-0	[S8]	Size of PCR product across T-DNA insertion site

Supplemental Experimental Procedures

Plant Transformation

A. thaliana seeds were surface sterilized with 70% ethanol solution with 0.5% (v/v) Triton X-100 before sowing. Plants were grown in a walk-in growth chamber with 125 to 175 µmol m^{-2} s^{-1} light intensity, 16 hour light/ 8 hour dark, 65% humidity. *A. thaliana* plants were transformed using the floral dip method [S9]. Transgenic lines carrying one copy of either *gDM1-2xHA* (pEC209), *gDM2d-4xMyc* (pMD325), or *indDM1-HA* (pDT010) in Col-0 wild-type or mutant backgrounds were identified on soil treated with 0.183 g/l Basta (glufosinate) and further bred to homozygosity in T_3. The F_1 hybrids used in this study were generated by crossing T_3 homozygous lines carrying each construct. Multiple independent lines were crossed to ensure robustness of results.

The F_1 hybrids of *indDM1-HA* and *gDM2d-4xMyc* were grown at 23°C on Basta treated soil. Expression of *DM1-HA* was induced in 15-days-old seedlings by irrigation with 1% ethanol. Ethanol treatment was performed by one-time irrigation and plants were covered by a plastic dome for 72 h. When domes were removed, remaining liquid in the tray was discarded. Necrosis was scored 3 days after ethanol treatment. Leaf sampling for co-immunoprecipitation was done 18 days after ethanol treatment.

Molecular Cloning

Site-directed mutagenesis was carried out by introducing corresponding changes in the primers and overlapping PCR. Genomic constructs of *DM1*, *DM2d* and *DM2g* and of their mutant derivatives were cloned to binary vectors by using conventional restriction enzymes or Gateway LR Cloning Technology (Invitrogen, Carlsbad, CA, USA). Primary sequences of the genic regions in all binary clones were confirmed with Sanger sequencing. Overlapping PCR method was used to generate all chimeric constructs, except for the NB-ARC domain swap constructs of DM2d/g. Six codon changes between DM2d and DM2g were introduced by site-directed mutagenesis in these chimeras. All the constructs with information on binary vector origins and primers used for overlapping PCR are listed at the end of this section.

The binary constructs were transformed into *A. tumefaciens* strain ASE by electroporation and transformants were selected on 25 µg/mL kanamycin, 25 µg/mL chloramphenicol, 100 µg/mL spectinomycin (for pGWB or pZZ006 constructs), or with the three antibiotics plus 25 µg/mL tetracycline (for pGREEN-IIS with pSOUP helper plasmid) [S10-S12]. Presence of plasmids was confirmed by colony PCR.

Expression Analyses

Total RNA from leaves of 20 day-old plants was extracted using acidified phenol [S13]. 1 µg of total RNA was used for cDNA synthesis using RevertAid RT Kit (Thermo Scientific, Vilnius, Lithuania) according to the manufacturer's protocol. cDNA was synthesized from 1 µg of total RNA using the RevertAid RT Kit (Thermo Scientific, Vilnius, Lithuania). The experiment was conducted with three independent F_1 lines and their parents and three technical replicates for each line.

Oligonucleotide primers for quantitative real-time PCR of *PR1*, *NPR1*, *WRKY46*, and *TUB2* control are listed at the end of this section. A PCR reaction mix, consisting of 2 µL of 1:5 diluted cDNA template, 0.25 µL of each primer at 100 pM, and 5 µL of Maxima SYBR Green Mix (Invitrogen, Carlsbad, CA, USA) in a total volume of 10 µL was prepared in three technical replicates. Relative expression of each target gene was measured by normalizing

CT value of the target gene to that of *TUB2* (ΔCT). To quantify the relative expression of the target gene in F_1 generation of *gDM1-2xHA* x *gDM2d-4xMyc* in wild type, and mutants (*eds1-1*, *rar1-21*, *sgt1b* and *rbohD*), ΔCT, value of the target gene in F_1 was calibrated to that of one of the parents carrying only *gDM1-2xHA* (ΔΔCT). The experiment was carried out with three independent lines of F_1 and parents. Each dot in Figure 1B represents –(ΔΔCT) value from a technical replicate, and data points from a biological replicate are marked with same color.

Transient Expression and Conductivity Assay

N. benthamiana plants were grown at 23°C and four to five week-old plants were used for *Agrobacterium tumefaciens*-mediated transient expression. *A. tumefaciens* (strain ASE) carrying a binary construct was grown overnight at 28°C in an orbital shaker at 200 rpm/min in 50 mL of LB medium containing appropriate antibiotics to OD_{600} of 1.2 to 1.8. Bacterial cells were harvested and resuspended in the induction medium containing 10 mM MES pH 5.6, 10 mM $MgCl_2$ and 150 µM acetosyringone with adjusted OD_{600} of 0.35. For *indDM1-HA* (pDT010), OD_{600} of 0.13 was used. After two hours of incubation in induction media at 28°C with 200 rpm/min, two bacterial inocula were mixed at 1:1 volume ratio with the addition of 1/10 volume of *Agrobacteria* carrying P19 to suppress transgene silencing. Bacterial mixtures were manually infiltrated using a 1-mL needleless syringe.

Expression of *indDM1-HA* was induced at 18 hpi by irrigating plants with 1% ethanol. Treated plants were kept under a plastic dome for additional 18 hours. At 36 hpi, five leaf discs (each with a diameter of 8 mm) from each plant were collected and floated in 15 mL water for 30 min. The leaf discs were transferred into a 6 ml tube with fresh water. Conductivity of samples in each tube was measured (µS/cm) using an Orion Star™ Conductivity Meter (Thermo Scientific, Beverly, MA, USA), from 36.75 to 60.75 hpi for seven to nine time points. The assay was carried out in eight biological replicates (5 discs x 8 plants) per indicated combination, and was repeated twice. One representative dataset is presented in Figure 2. Statistical analysis was carried out using GraphPad Prism v6.0c.

For competition assays, increasing amounts of the competitor inoculum (*A. tumefaciens* transformed with DT100, DT182, MD365 or MD366) were co-infiltrated with a premixed aliquot of DM1- and DM2d-expression constructs (EC209 and MD325). Before mixing, OD_{600} of each competitor was 0.525, 1.05 and 2.1, and of DM1 and DM2d were 0.525. Conductivity was measured from 43 hpi onward at five time points.

Yeast Two-Hybrid Assay

The Matchmaker GAL4 Two-Hybrid Systems (Clontech, Mountain View, CA, USA) was used with *Saccharomyces cerevisiae* strain AH109. Growth assays on minimal yeast media used 1:10 serial dilutions starting with OD_{600} of 0.5. At least four individual clones were used per assay and two independent assays were performed.

Yeast cells, grown from a colony in YPD medium at 30°C overnight, were harvested by centrifugation and lysed by a repetitive freezing and thawing for two minutes each. The crude protein extract was resuspended in 50 µL of 3X urea Laemmli buffer (240 mM Tris-HCl pH 6.8, 6% SDS, 30% glycerol, 16% β-mercaptoethanol, 0.006% bromophenol blue, 10 M Urea), denatured by boiling for 15 minutes, separated on 10% SDS-PAGE gel and immunoblotted on PVDF membrane (Bio-Rad, Foster City, CA, USA). AD- or BD-binding proteins were detected by anti-HA-peroxidase (Roche, Mannheim, Germany) (1:5,000 dilution), anti-c-Myc-horseradish peroxidase (HRP) (Sigma-Aldrich, Saint Louis, MO, USA) (1:15,000 dilution) or anti-GAL4 (DBD) (Santa Cruz Biotechnology, Dallas, TX, USA)

(1:1,000 dilution). Information on the control Y2H interaction (AD:RGL3 and BD:AP1) can be found [S14]**.**

Protein Expression in Plants

Microsomal fractions of the samples were prepared according to the reported method [S15] with the following modification. 100 mg leaf tissue was ground into fine powder in liquid nitrogen and homogenized in 210 µL of lysis buffer (0.33 M sucrose, 20 mM Tris-HCl pH 7.5, 1 mM EDTA, 10 mM DTT and 1 x cOmplete ULTRA Tablets, Mini, EDTA-free protease inhibitor cocktail (Roche). The lysate was cleared by a table-top centrifugation at 5,000 x g for 10 min at 4°C, and microsomal pellet fractions were collected by centrifugation at 20,000 g for 1 h at 4°C. Extracted proteins were resuspended in 2 x Laemmli sample buffer, boiled for 10 min at 95°C, separated on 7% SDS-PAGE gel and immunoblotted on PVDF membrane. The membrane was incubated with anti-c-Myc-HRP (Sigma-Aldrich) (1:15,000 dilution), or anti-HA-peroxidase (Roche) (1:5,000 dilution).

For co-immunoprecipitation assays, 500 mg of *N. benthamiana* or 1 g of *A. thaliana* leaf tissue was ground into fine powder in liquid nitrogen, and homogenized in 1 mL of extraction buffer (50 mM HEPES-KOH pH 7.5, 50 mM NaCl, 10 mM EDTA pH 8.0, 10 mM $MgCl_2$, 0.5% Tween-20, 5 mM DTT, 1x cOmplete ULTRA Tablets, Mini, EDTA-free protease inhibitor cocktail). The lysates were cleared by centrifugation at 10,000 g for 10 min at 4°C. 25 µL of Pierce™ anti-c-Myc magnetic beads or Pierce™ anti-HA magnetic beads (Thermo Scientific, Rockford, IL, USA) after equilibrating in the extraction buffer were mixed with the supernatants. After incubation for 4 hours at 4°C, the magnetic beads were collected and washed 3 times with washing buffer (same to the extraction buffer but containing 0.2% Tween-20). Bound proteins were collected by adding 50 µL of pre-heated elution buffer (50 mM Tris-HCl pH 6.8, 50 mM DTT, 1% SDS, 1 mM EDTA pH 8.0, 0.005% bromophenol blue, 10% glycerol). The immunoprecipitated proteins from anti-c-Myc were loaded on a 7% SDS-PAGE gel and detected after blotting with anti-c-Myc HRP (Sigma-Aldrich) (1:15,000 dilution) and anti-HA-peroxidase (Roche) (1:5,000 dilution).

BN-PAGE that we used to monitor DM1 and/or DM2d/g-containing protein complexes in *A. thaliana* essentially followed the protocol described in [S16]. The relative molecular weights of protein complexes were determined by loading 5 µl of NativeMark unstained protein ladder (ThermoFischer, Madison, WI. USA).

Binary T-DNA Constructs

Construct	Backbone	Promoter	Coding region
pDT010	pZZ006*	*palcA*	*DM1-2xHA*
pDT077	pGREENIIS	*pDM2d*	*TIR(DM2d)-NB(DM2g)-LRR(DM2d)-4xMyc*
pDT081	pGREENIIS	*pDM2d*	*TIR(DM2g)-NB(DM2d)-LRR(DM2d)-4xMyc*
pDT092	pGREENIIS	*p35S*	*DM2g-4xMyc*
pDT100	pGREENIIS	*pDM2d*	*DM2g-4xMyc*
pDT101	pGREENIIS	*pDM2d*	*TIR(DM2g)-NB(DM2d)-LRR(DM2g)-4xMyc*
pDT103	pGREENIIS	*pDM2d*	*TIR(DM2d)-NB(DM2g)-LRR(DM2g)-4xMyc*
pDT105	pGREENIIS	*pDM2d*	*DM2d$^{1-581}$-4xMyc*
pDT134	pGREENIIS	*pDM1*	*DM1^{H491V}-2xHA*
pDT135	pGREENIIS	*pDM1*	*DM1$^{G223A\ K224A\ H491V}$-2xHA*
pDT137	pGREENIIS	*pDM1*	*DM1^{G31R}-2xHA*
pDT138	pGREENIIS	*pDM1*	*DM1^{G31T}-2xHA*
pDT139	pGREENIIS	*pDM1*	*DM1^{G31D}-2xHA*
pDT140	pGREENIIS	*pDM1*	*DM1^{G31E}-2xHA*
pDT143	pGREENIIS	*pDM2d*	*DM2d^{T66A}-2xHA*
pDT144	pGREENIIS	*pDM2d*	*DM2d^{T66G}-2xHA*
pDT157	pGREENIIS	*pDM1*	*DM1$^{1-218}$-2xHA*
pDT158	pGREENIIS	*pDM2d*	*DM2d$^{1-254}$-4xMyc*
pDT164	pZZ006	*palcA*	*DM1$^{G223A\ K224A}$-2xHA*
pDT165	pZZ006	*palcA*	*DM1^{H491V}-2xHA*
pDT166	pZZ006	*palcA*	*DM1$^{G223A\ K224A\ H491V}$-2xHA*
pDT182	pGREENIIS	*pDM1*	*DM1$^{Col\text{-}0|495\text{-}988}$-2xHA*
pDT186	pGREENIIS	*pDM1*	*DM1^{H491T}-2xHA*
pDT187	pGREENIIS	*pDM2d*	*DM2d^{T541H}-4xMyc*
pDT192	pGREENIIS	*pDM1*	*DM1$^{1-528}$-2xHA*
pDT193	pGREENIIS	*pDM2d*	*DM2d/g (LRR swap 1)-4xMyc*
pDT194	pGREENIIS	*pDM2d*	*DM2d/g (LRR swap 2)-4xMyc*
pDT195	pGREENIIS	*pDM2d*	*DM2d/g (LRR swap 3)-4xMyc*
pDT196	pGREENIIS	*pDM2d*	*DM2d/g (LRR swap 4)-4xMyc*
pDT197	pGREENIIS	*pDM2d*	*DM2d/g (LRR swap 5)-4xMyc*
pDT198	pGREENIIS	*pDM2d*	*DM2d/g (LRR swap 6)-4xMyc*

pDT207	pGREENIIS	*pDM2d*	*TIR(DM2d)-NB(DM2d)-LRR(DM2g)-4xMyc*
pDT208	pGREENIIS	*pDM2d*	*TIR(DM2g)-NB(DM2g)-LRR(DM2d)-4xMyc*
pEC209	pGREENIIS	*pDM1*	*DM1-2xHA*
pEC300	pGWB420	*p35S*	*DM2d$^{1-358}$-10xMyc*
pMD324	pGREENIIS	*pDM2d*	*DM2d-2xHA*
pMD325	pGREENIIS	*pDM2d*	*DM2d-4xMyc*
pMD341	pGWB414**	*p35S*	*DM1$^{529-1067}$-3xHA*
pMD344	pGWB420	*p35S*	*DM1$^{687-1216}$-10xMyc*
pMD347	pGWB420	*p35S*	*DM2g-10xMyc*
pMD365	pGREENIIS	*pDM1*	*DM1$^{G223A\ K224A}$-2xHA*
pMD366	pGREENIIS	*pDM2d*	*DM2d$^{G259A\ K260A}$-4xMyc*
pMD444	pGREENIIS	*pDM1*	*DM1$^{1-308}$-2xHA*
pMD445	pGREENIIS	*pDM2g*	*DM2g-4xMyc*
pMD447	pGWB416	*pDM1*	*DM1-4xMyc*
pMD469	pGREENIIS	*pDM2d*	*DM2d^{T541V}-4xMyc*
pMD470	pGREENIIS	*pDM2d*	*DM2d^{T541D}-4xMyc*
pMD471	pGREENIIS	*pDM2d*	*DM2d$^{G259A\ K260A\ T541V}$-4xMyc*
pMD477	pGREENIIS	*pDM1*	*DM1$^{S34A\ H35A}$-2xHA*
pMD478	pGREENIIS	*pDM2d*	*DM2d$^{S69A\ H70A}$-4xMyc*

*pZZ006 incorporates ethanol-inducible AlcR transcription factor-*alcA* promoter system from *Aspergillus nidulans* [S17] into pMLBart binary backbone [S12].

**pGWB vectors are from [S10]

Oligonucleotide Primers for DM2d/DM2g Chimeras and Site-directed Mutagenesis

Primer	Purpose	Orientation	Sequence
G-38231	NB-ARC swap II	Forward	ATGAGATTGCTTGGGAAGTTACCTGCT TAGCTGGTAAACTCCCTTTGGGAT
G-38232	NB-ARC swap II	Reverse	ATCCCAAAGGGAGTTTACCAGCTAAGC AGGTAACTTCCCAAGCAATCTCAT
G-38233	NB-ARC swap II	Forward	TGAAGTGCTCAATGATGATACAATAGT AAGTTTTTTCA
G-38234	NB-ARC swap II	Reverse	TGAAAAAACTTACTATTGTATCATCATT GAGCACTTCA
G-38410	NB-ARC swap I	Forward	CACGAAGGTTTCGATGAGATTGCAAGG GAAGTTATGGCCCTTGCTGGTGAACTC CCTTTGGGATTGAAGGTTCTAGGC
G-38411	NB-ARC swap I	Reverse	GCCTAGAACCTTCAATCCCAAAGGGAG TTCACCAGCAAGGGCCATAACTTCCCT TGCAATCTCATCGAAACCTTCGTG
G-38412	NB-ARC swap I	Forward	GAAAGGGATATATGTGAAGTACTCGAT GACGATACAACAGTAAGTTTTTTCATTG CATCTC
G-38413	NB-ARC swap I	Reverse	GAGATGCAATGAAAAAACTTACTGTTG TATCGTCATCGAGTACTTCACATATATC CCTTTC
G-38521	TIR and LRR swap	Forward	CTAATGGATTCTTCTTTTTTCCTTGTCT TAGT
G-38522	TIR and LRR swap	Reverse	ACTAAGACAAGGAAAAAAGAAGAATCC ATTAG
G-38523	TIR and LRR swap	Forward	ATGGTTTTGTTGGGATGACACCTCATA TGG
G-38524	TIR and LRR swap	Reverse	CCATATGAGGTGTCATCCCAACAAAAC CAT
G-39654	LRR swap 1-6	Forward	CTTGATAATTGAGTTTATTTGATAAC
G-39655	LRR swap 1-6	Reverse	GTTATCAAATAAACTCAATTATCAAG
G-39656	LRR swap 1, 4	Forward	CTAAAGTAAGTAGTTTTGATGAAAACT
G-39657	LRR swap 1, 4	Reverse	AGTTTTCATCAAAACTACTTACTTTAG
G-39658	LRR swap 2, 5	Forward	GTCTCTAAGAAATTGTTCACGTGTTGT
G-39659	LRR swap 2, 5	Reverse	ACAACACGTGAACAATTTCTTAGAGAC
G-39660	LRR swap 3, 6	Forward	GCTAGAGACTCTTCCAATCAACATC

G-39661	LRR swap 3, 6	Reverse	GATGTTGATTGGAAGAGTCTCTAGC
G-39662	LRR swap 4, 5, 6	Reverse	GAATTGGGTAGCGGCCGCCCCCTCGAGC

Oligonucleotide Primers for qRT-PCR

Primer	Gene	Orientation	Sequence
N-0078	*TUB2*	Forward	GAGCCTTACAACGCTACTCTGTCTGTC
N-0079	*TUB2*	Reverse	ACACCAGACATAGTAGCAGAAATCAAG
G-13182	*PR1*	Forward	CGTTCACATAATTCCCACGA
G-13183	*PR1*	Reverse	AAGAGGCAACTGCAGACTCA
G-13184	*NPR1*	Forward	CGTTTCTCAGCAGTGTCGTC
G-13185	*NPR1*	Reverse	CCGTCTCACTGGTACGAAGA
G-38254	*WRKY46*	Forward	CGTGCATCTGTAATATGCTCTAGG
G-38255	*WRKY46*	Reverse	GATGATGGTCACTGCTGGAG
G-29987	*DM1-2xHA*	Forward	CCAAGTGGGCAACTTTGAAT
G-36197	*DM1-2xHA*	Reverse	AGCTGCATAGTCCGGGACGTC
G-23330	*DM2d-4xMyc*	Forward	CACCAAGCGAGCATGAGATA
G-31100	*DM2d-4xMyc*	Reverse	CTAAGCGCTACCGTTCAAGTCT

Supplemental References

S1. Bomblies, K., Lempe, J., Epple, P., Warthmann, N., Lanz, C., Dangl, J.L., and Weigel, D. (2007). Autoimmune response as a mechanism for a Dobzhansky-Muller-type incompatibility syndrome in plants. PLoS Biol. *5*, e236.

S2. Schreiber, K.J., Bentham, A., Williams, S.J., Kobe, B., and Staskawicz, B.J. (2016). Multiple domain associations within the Arabidopsis immune receptor RPP1 regulate the activation of programmed cell death. PLoS Pathog. *12*, e1005769.

S3. Hu, Z., Yan, C., Liu, P., Huang, Z., Ma, R., Zhang, C., Wang, R., Zhang, Y., Martinon, F., Miao, D., et al. (2013). Crystal structure of NLRC4 reveals its autoinhibition mechanism. Science *341*, 172-175.

S4. Kelley, L.A., Mezulis, S., Yates, C.M., Wass, M.N., and Sternberg, M.J. (2015). The Phyre2 web portal for protein modeling, prediction and analysis. Nat Protoc *10*, 845-858.

S5. Parker, J.E., Holub, E.B., Frost, L.N., Falk, A., Gunn, N.D., and Daniels, M.J. (1996). Characterization of *eds1*, a mutation in Arabidopsis suppressing resistance to *Peronospora parasitica* specified by several different *RPP* genes. Plant Cell *8*, 2033-2046.

S6. Tornero, P., Merritt, P., Sadanandom, A., Shirasu, K., Innes, R.W., and Dangl, J.L. (2002). *RAR1* and *NDR1* contribute quantitatively to disease resistance in Arabidopsis, and their relative contributions are dependent on the *R* gene assayed. Plant Cell *14*, 1005-1015.

S7. Tör, M., Gordon, P., Cuzick, A., Eulgem, T., Sinapidou, E., Mert-Turk, F., Can, C., Dangl, J.L., and Holub, E.B. (2002). Arabidopsis SGT1b is required for defense signaling conferred by several downy mildew resistance genes. Plant Cell *14*, 993-1003.

S8. Alonso, J.M., Stepanova, A.N., Leisse, T.J., Kim, C.J., Chen, H., Shinn, P., Stevenson, D.K., Zimmerman, J., Barajas, P., Cheuk, R., et al. (2003). Genome-wide insertional mutagenesis of *Arabidopsis thaliana*. Science *301*, 653-657.

S9. Clough, S.J., and Bent, A.F. (1998). Floral dip: a simplified method for *Agrobacterium*-mediated transformation of *Arabidopsis thaliana*. Plant J. *16*, 735-743.

S10. Nakagawa, T., Suzuki, T., Murata, S., Nakamura, S., Hino, T., Maeo, K., Tabata, R., Kawai, T., Tanaka, K., Niwa, Y., et al. (2007). Improved Gateway binary vectors: high-performance vectors for creation of fusion constructs in transgenic analysis of plants. Biosci. Biotechnol. Biochem. *71*, 2095-2100.

S11. Hellens, R.P., Allan, A.C., Friel, E.N., Bolitho, K., Grafton, K., Templeton, M.D., Karunairetnam, S., Gleave, A.P., and Laing, W.A. (2005). Transient expression vectors for functional genomics, quantification of promoter activity and RNA silencing in plants. Plant Methods *1*, 13.

S12. Zhao, Z., Andersen, S.U., Ljung, K., Dolezal, K., Miotk, A., Schultheiss, S.J., and Lohmann, J.U. (2010). Hormonal control of the shoot stem-cell niche. Nature *465*, 1089-1092.

S13. Box, M.S., Coustham, V., Dean, C., and Mylne, J.S. (2011). Protocol: A simple phenol-based method for 96-well extraction of high quality RNA from Arabidopsis. Plant Methods *7*, 7.

S14. Yu, S., Galvao, V.C., Zhang, Y.C., Horrer, D., Zhang, T.Q., Hao, Y.H., Feng, Y.Q., Wang, S., Schmid, M., and Wang, J.W. (2012). Gibberellin regulates the Arabidopsis floral transition through miR156-targeted SQUAMOSA promoter binding-like transcription factors. Plant Cell *24*, 3320-3332.

S15. Boyes, D.C., Nam, J., and Dangl, J.L. (1998). The *Arabidopsis thaliana RPM1* disease resistance gene product is a peripheral plasma membrane protein that is degraded coincident with the hypersensitive response. Proc. Natl. Acad. Sci. USA *95*, 15849-15854.

S16. Klodmann, J., Senkler, M., Rode, C., and Braun, H.P. (2011). Defining the protein complex proteome of plant mitochondria. Plant Physiol. *157*, 587-598.

S17. Caddick, M.X., Greenland, A.J., Jepson, I., Krause, K.-P., Qu, N., Riddell, K.V., Salter, M.G., Schuch, W., Sonnewald, U., and Tomsett, A.B. (1998). An ethanol inducible gene switch for plants used to manipulate carbon metabolism. Nat. Biotechnol. *16*, 177-180.